

# LETTERS TO THE EDITOR

## ASTROPHYSICS

### Oscillation Periods of Neutron Stars

THE recent discovery<sup>1-4</sup> of celestial X-ray sources prompted various authors<sup>5-12</sup> to propose possible production mechanisms of these X-rays. In an earlier communication, one of us<sup>12</sup> suggested that some of the X-ray emission might be associated with the mechanical energy of radial oscillations of neutron stars. To investigate such a possibility, precise knowledge of the oscillation periods is important. The investigation of the possible effect of nuclear forces on such periods is interesting in itself. This communication presents some results of such work.

It is well known that general relativity is important in such condensed bodies as neutron stars. Therefore, the circular frequency for purely radial oscillations in general relativity, as given by Chandrasekhar<sup>13-15</sup> (the final corrected expression), was used in our calculations. Three types of nuclear forces were chosen for use in the equation of state. One, designated 'Skyrme', is a three-body nuclear potential<sup>16</sup>. The other two are neutron-neutron potentials derived by Levinger and Simmons<sup>17</sup>, and are designated  $V_\beta$  and  $V_\gamma$  potentials. The case of non-interacting fermions was also considered for comparison. The models with zero interactions are designated 'ideal' gas models, and the others with the three types of nuclear forces are called the 'Skyrme',  $V_\beta$  and  $V_\gamma$  type models, respectively. The properties of these models are more fully described in a thesis<sup>11</sup>, and will be published in due course.

The periods for the four kinds of models are shown as a function of the stellar gravitational mass in Fig. 1; the periods are expressed in milliseconds and the masses are expressed in solar mass units. The broad horizontal portion of each curve corresponds to a series of stable neutron star models. The 'Skyrme'-type stars have periods of 0.2-0.3 msec and the  $V_\gamma$  type stars have periods of 0.4-0.5 msec in the stable region. The typical periods of the  $V_\beta$  type models are about 0.3 msec when the stars are massive, but for less-massive models the periods are about 1 msec. The periods for ideal gas models vary rapidly with mass, decreasing with increasing mass to about 0.8 msec. Estimates of oscillation periods that can be

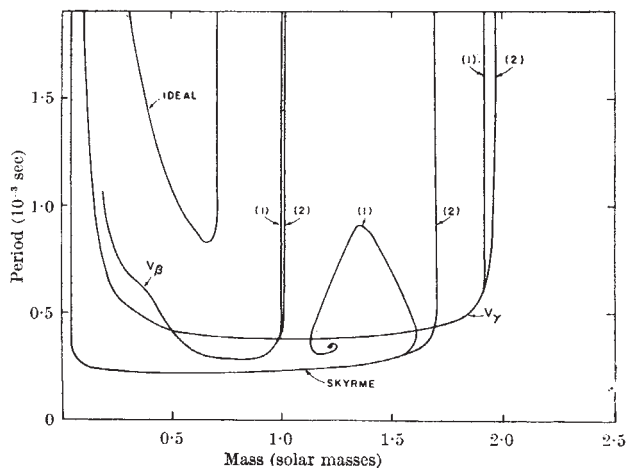


Fig. 1. Periods of radial oscillation for neutron stars corresponding to four equations of state. The branches marked (1) represent equations of state limited so that the pressure does not exceed one third of the proper energy density; branches marked (2) are limited so that the pressure does not exceed the proper energy density

obtained from the classical equations (order of msec)<sup>18</sup> are especially good for the ideal gas models. However, our present results show that we must resort to calculations of the exact general relativistic expressions to obtain more detailed quantitative information.

In a suitable equation of state the pressure is not allowed to increase without limit as the density increases, so that either the restriction  $p \leq \epsilon/3$  or  $p \leq \epsilon$  must be imposed. The periods were calculated for both restrictions on the equations of state and are shown in Fig. 1. The curves denoted by (1) represent the models with the limit  $p \leq \epsilon/3$  and those by (2) with  $p \leq \epsilon$ . The difference is negligible over the major portion of the stable region because these restrictions become applicable only near the massive end of the stability region for some of the equations of state used.

The square of frequency  $\omega^2$  is positive in a stable region, becomes zero at the point of instability, and is negative in the region of instability<sup>13-15</sup>. The period approaches infinity at the boundaries of the stable region (one or both ends of the curves in Fig. 1). The curve of the 'Skyrme'-type models with  $p \leq \epsilon/3$ , however, fails to show this singularity at the massive end. Instead of going to infinity (that is,  $\omega^2 = 0$ ), the period approaches a finite value, as infinite central density is approached, after a number of damped oscillations. For this particular model, instability never sets in at the high-density limit. All other models chosen for this investigation, however, show a singularity at the point of the major mass maximum.

The behaviour on the low-mass side is more complicated. In order to obtain more quantitative information in this region we must include electrons in our configuration. All present models have a pure neutron configuration. Therefore, all curves in Fig. 1 are terminated near 0.2 solar masses.

In order to single out the effect of nuclear forces on the periods, the following period normalization may be used. The normalization factor,  $\tau_n$ , is defined as:

$$\tau_n = 2\pi/\omega_n,$$

where:

$$\omega_n^2 = AGMR^{-3} \left[ 3\Gamma - 4 - 3GM/c^2 R^{-1} \left( \frac{10}{7} \Gamma - 1 \right) \right]. \quad (1)$$

The formula for  $\omega_n^2$  is the expression obtained for a homogenous fluid sphere with a constant  $\Gamma$  and constant energy density, if one expands the formula<sup>5</sup> for  $\omega^2$ , subject to the condition  $2GM/c^2 R < 1$ . The third term in the expression is therefore the general relativistic effect (this expression is quite general and may be used for any range of mass), and the general relativistic effect on the periods is accounted for in this way. The factor  $A$  is a correction which accounts for the departure from homogeneity, and  $\Gamma$  is the ratio of specific heats.

In Fig. 2, the normalized periods,  $\tau/\tau_n$  (with  $\Gamma = 5/3$  and  $A = 1$ ), are plotted versus stellar mass. We note that the effects of nuclear forces are shown more clearly in this figure. Near ordinary nuclear densities the 'Skyrme'-type potential has the largest attractive term, which decreases the pressure at a given density, the  $V_\gamma$  type has an attractive term of intermediate magnitude, and the  $V_\beta$  type has the least attractive term. One conclusion to be drawn from Fig. 2 is that an attractive force tends to decrease the oscillation periods.

The calculations presented here are intended only to illustrate the importance of nuclear interaction corrections to the equation of state. It seems likely that neutron star vibration periods will be less than would be calculated for a gas of non-interacting particles. If thermal emission

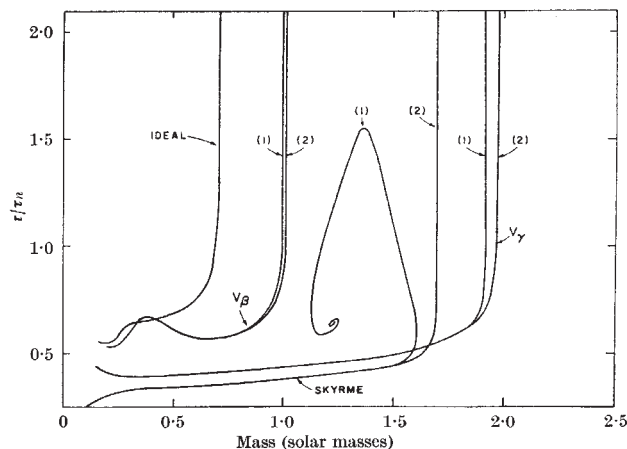


Fig. 2. Periods of radial oscillation of neutron stars with four equations of state relative to the normalization factor  $\tau_n$ , defined in equation 1. The branches marked (1) and (2) are as defined for Fig. 1

in the soft X-ray region should be detected from such objects, then it will become desirable to attempt to detect and measure vibration periods. With some additional indication of the mass or radius of such objects, these periods will then give information about the nuclear forces in the interiors of neutron stars.

SACHIKO TSURUTA  
JAMES P. WRIGHT

Smithsonian Astrophysical Observatory,  
Cambridge, Massachusetts.

A. G. W. CAMERON

Institute for Space Studies,  
Goddard Space Flight Center,  
National Aeronautics and Space Administration,  
New York.

<sup>1</sup> Giacconi, R., Gursky, H., Paolini, F. R., and Rossi, B. B., *Phys. Rev. Letters*, **9**, 439 (1962).

<sup>2</sup> Giacconi, R., Gursky, H., Paolini, F. R., and Rossi, B. B., *Phys. Rev. Letters*, **11**, 530 (1963).

<sup>3</sup> Bowyer, S., Byram, E. T., Chubb, T. A., and Friedman, H., *Nature*, **201**, 1307 (1964).

<sup>4</sup> Fisher, P. C., and Meyerott, A. F., *Astrophys. J.*, **139**, 123 (1964).

<sup>5</sup> Chiu, H. Y., and Salpeter, E. E., *Phys. Rev. Letters*, **12**, 412 (1964).

<sup>6</sup> Morton, D. C., *Nature*, **201**, 1308 (1964).

<sup>7</sup> Misner, C. W., and Zapsolsky, H. S., *Phys. Rev. Letters*, **12**, 635 (1964).

<sup>8</sup> Finzi, A., *Astrophys. J.*, **139**, 1398 (1964).

<sup>9</sup> Morrison, P., Second Texas Symp. on Relativistic Astrophysics, Austin, 1964 (to be published).

<sup>10</sup> Burbidge, G. R., Gould, R. T., and Tucker, W. H., *Phys. Rev. Letters*, **14**, 289 (1965).

<sup>11</sup> Tsuruta, S., thesis, Columbia Univ. (1964).

<sup>12</sup> Cameron, A. G. W., *Nature*, **205**, 787 (1965).

<sup>13</sup> Chandrasekhar, S., *Astrophys. J.*, **140**, 417 (1964).

<sup>14</sup> Chandrasekhar, S., *Phys. Rev. Letters*, **12**, 114 (1964).

<sup>15</sup> Chandrasekhar, S., *Phys. Rev. Letters*, **12**, 437 (1964).

<sup>16</sup> Skyrme, T. H. R., *Nuclear Phys.*, **9**, 615 (1959).

<sup>17</sup> Levinger, J. S., and Simmons, L. M., *Phys. Rev.*, **124**, 916 (1961).

<sup>18</sup> Rosseland, S., *The Pulsation Theory of Variable Stars* (Clarendon Press, Oxford, 1949).

### Visible Polarization Data of Mars

FOR several years the most widely accepted value of 90 mbar for the surface pressure on Mars had been based on visible photometric and polarimetric work, particularly by Dollfus<sup>1</sup> (cf. de Vaucouleurs<sup>2</sup> for a detailed discussion). Recently, however, a value of  $25 \pm 15$  mbar has been derived by Kaplan, Münch, and Spinrad<sup>3</sup> from a curve-of-growth analysis of pressure-broadened carbon-dioxide vibration-rotation lines in near infra-red Martian spectra. A possible explanation of the discrepancy is that aerosol particles in the Martian atmosphere contribute an appreciable component to the observed brightness and polarization of Mars. Dollfus assumed that Rayleigh scattering by molecules dominates the atmospheric brightness and polarization at  $\lambda$  6100 Å and that the aerosol contribution

is insignificant. If this is not the case, then certain important deductions may have to be changed. The purpose of this communication is to illustrate what these changes may be.

Using four different methods based on polarization and brightness measures of Mars, Dollfus<sup>1</sup> derived for  $\lambda$  6100 Å a ratio of the atmospheric brightness to the surface brightness,  $B_a/B_s = 0.028$ , for the bright areas at the centre of the Martian disk at zero phase (opposition). Applying the expression for Rayleigh scattering, and assuming that the scattering properties of the atmospheric gases of Mars and Earth are similar, he arrived at a surface pressure of 90 mbar. But if the surface pressure were 25 mbar, the ratio  $B_a/B_s$  would be only 0.0078 on the basis of molecular scattering. A significant portion of the rest of the atmospheric brightness may reasonably be attributed to scattering by aerosol particles. We will arbitrarily assume that  $B_a/B_s = 0.028$  and  $P = 25$  mbar, so that the brightness of the aerosols is 65/25 that of the gas.

The next step in determining the contribution of the aerosol component to the total polarization of Mars is to examine the polarizations by various compositions, shapes, sizes, and size distributions of the particles. Kuiper<sup>4</sup> has suggested that spherical ice particles of submicron size can explain the ultra-violet polarimetric, photometric, and photographic properties of the Martian blue haze. For the scattering of visible radiation by spherical particles of such sizes, one must resort to Mie scattering theory, in which the polarization and brightness properties of an atmosphere depend on the parameter  $x = 2\pi a/\lambda$ , where  $a$  is the particle radius and  $\lambda$  the wavelength of observation. Computations of polarization and intensity versus phase angle for various distributions of  $x$  have been carried out by B. M. Herman and are cited by Kuiper<sup>4</sup>. We have selected two of his "balanced" mixtures, A" and B" (neither integral nor half-integral values of  $x$  are favoured), which would apply to  $\lambda$  6100 Å for most frequent diameters of 0.58 and 0.77  $\mu$  respectively (Table 1).

The curves of the polarization versus phase angle for these mixtures are shown in Fig. 1b, c. These polarizations exhibit a strong negative branch at low phase angles and cross-over from negative to positive polarizations between 30° and 40°. This behaviour is quite different from that of molecular polarization, Fig. 1a, which is always positive and increases with the phase angle.

We next computed the total atmospheric polarization versus phase angle for these mixtures for a 25 mbar atmosphere, Fig. 1d, e. This is easily done using the formula:

$$P_a = \frac{P_p B_p + P_m B_m}{B_p + B_m}$$

where  $P_a$  is the total atmospheric polarization,  $P_p$  the polarization by aerosol particles,  $B_p$  the particle brightness,  $P_m$  the molecular polarization, and  $B_m$  the molecular brightness.  $P_p$  and  $B_p$  versus phase angle are given by Kuiper<sup>4</sup>, and  $P_m$  and  $B_m$  versus phase angle are calculated from the well-known expressions for Rayleigh scattering.  $B_p + B_m$  is normalized to unity at zero phase angle with relative weights of 65 and 25 for  $B_p$  and  $B_m$  respectively.

To satisfy ourselves that it is reasonable to propose that aerosols contribute as much as 65/90 of the atmospheric brightness at  $\lambda$  6100 Å, we computed the required abundances of mixtures A" and B". With the assumption of the similarity of the scattering properties of the terrestrial and Martian atmospheric constituents the results are about  $2 \times 10^6$  particles  $\text{cm}^{-2}$  for mixture A" and about  $1 \times 10^6$  particles  $\text{cm}^{-2}$  for mixture B". For

Table 1. THE WEIGHTING FACTORS FOR THE AEROSOL MIXTURES A" AND B"

Mixture/x	2.0	2.5	3.0	3.5	4.0	4.5	5.0	5.5
A"	2	7	10	7	2	0	0	0
B"	0	0	2	7	10	7	2	0